International Journal of Innovative
Computing, Information and Control
Volume **9**, Number **1**, January **2013**

ICIC International ©2013 ISSN 1349-4198
pp. **387–396**

MOTION CONTROL OF A WHEELED MOBILE ROBOT USING DIGITAL ACCELERATION CONTROL METHOD

Yina Wang, Shuoyu Wang, Renpeng Tan and Yinlai Jiang

School of Systems Engineering
Kochi University of Technology
185 Miyanokuchi, Tosayamada, Kami, Kochi 782-8502, Japan
{ 156013z; 138003t }@gs.kochi-tech.ac.jp; { wang.shuoyu; jiang.yinlai }@kochi-tech.ac.jp

Received October 2011; revised February 2012

Abstract. *Wheeled mobile robots are widely used in industry, ports, and agriculture because they have the necessary loading capability. High performance path-tracking is very important for the mobile robot to precisely follow the designed cargo-carrying path. However, the mobile robot sometimes strays from the predefined path because of center-of-gravity (COG) shifts, load changes caused by loads, and nonlinear friction in the wheels. To address these issues, a dynamics model, which considers COG shifts, load changes, and nonlinear friction, is derived and a digital acceleration control algorithm is proposed for the mobile robot. Simulations are executed using the proposed method and the results demonstrate the feasibility and effectiveness of the proposed digital acceleration control method by comparing with a proportional-integral (PI) controller.*
Keywords: Wheeled mobile robot, Nonlinear friction, Motion control, Digital acceleration control, Path-tracking

1. **Introduction.** Wheeled mobile robots are widely used in industry, ports and agriculture, because they have the necessary loading capability. Using wheeled mobile robots is an effective way to promote the factory automation [1]. As an example, the mobile robots with intelligent motion function are effective to improve the efficiency of cargo transport in factory automation and outdoor environments [2]. In cargo-transport task, the robots move to the target location following their predefined path. It is essential for these robots to precisely track the predefined path from the starting location to the target location, carrying as much cargo as possible and transport the cargo at a high speed. However, because of the center-of-gravity (COG) shifts and load changes caused by large loads and the serious nonlinear friction at the high speed, the accuracy of the path-tracking decreases and the robots stray from the predefined path, which clearly increases the danger of hitting obstacles. Therefore, motion control is one of the most fundamental topics for mobile robots. When the problem of COG shifts, load changes and nonlinear friction is solved, the motion performance of the wheeled mobile robots will be further improved to realize reliable and efficient cargo-transport.

Various researches focusing on the motion control of these mobile robots have been conducted. The work in [3] presents an overview of the control design trends for mobile robots. [4] provides a generic path following control strategy that is quite robust to measurement errors and external disturbances, and a time-varying control method and a nonsmooth feedback control strategy are proposed in [5,6] to address the problem of stabilization obstruction. However, these controllers are only effective to the bounded nonlinear friction and cannot deal with the problem of COG shifts and load changes. A control strategy that integrates a kinemics controller and an adaptive wavelet neural

network controller has been proposed for mobile robots, recently. Learning the parameters of the plant on line based on an adaptive learning algorithm, this controller is effective to deal with the problem of the COG shifts and load changes. It is also effective to deal with the bounded disturbance by using a robust term. Most of the previous controllers have achieved good path-tracking performance for the mobile robots. However, the existent controllers are only effective to compensate given or bounded friction by properly tuning the control parameters. In practice, the nonlinear friction of mobile robots is uncertain or unbounded due to the different working environment with different kinds of grounds. When the nonlinear friction has a change and the change is out of the permitted scope, these controllers are not effective anymore, and the tracking performance is insufficient.

Researchers in [7] focused on the motion process of mechanical systems and proposed a motion control method to deal with the nonlinear friction of a robot manipulator. The effectiveness of this method was demonstrated by experiment [8]. This method is now widely known as the digital acceleration control method [9]. Based on these previous studies, a digital acceleration control method to compensate the nonlinear friction for the mobile robot has been proposed in [10]. This control method is based on the thought that the nonlinear friction is contained in the control input by using the digital acceleration signal. The most significant advantage of this method is that, the control input is theoretically effective to deal with the nonlinear friction even if it is uncertain or unbounded due to the different working environment with different kinds of grounds.

In this paper, we utilize the digital acceleration control method proposed in [10] for the path-tracking of the mobile robot. The proposed control method improves the accuracy of the path-tracking by compensation of the COG shifts, load changes and nonlinear friction. Firstly, the design of the structure, the kinematic and dynamic analysis of the wheeled mobile robot are described. Then, a detailed description of the digital acceleration controller, and a stability proof of the control system are given. Finally, circular simulations of the proposed digital acceleration controller are conducted. The simulation results demonstrate the feasibility and effectiveness of the proposed control method by comparing it with a PI controller.

2. **Structure of the Mobile Robot and Modeling.** The mobile robot studied in this paper is shown in Figure 1. It has two driving wheels and two free casters.

FIGURE 1. Mobile robot

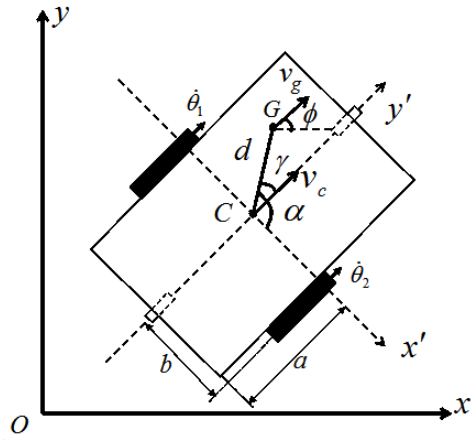

FIGURE 2. Structural model of the mobile robot

To develop the control law for the mobile robot, the necessary kinematic and dynamic equations are derived based on the coordinate systems and the structural model shown in Figure 2.

The parameters and coordinate systems are as follows:

$\Sigma(x, y, O)$: Absolute coordinate system;

$\Sigma(x', y', C)$: Translation coordinate system determined by the movement direction of the mobile robot;

$G(x_g, y_g)$: Position of the COG considering the effect of the loads;

$C(x_c, y_c)$: Position of the geometric center of the mobile robot;

v_c: Velocity at geometric center C;

ϕ: The orientation angle between the direction of v_c and the x-axis;

$\dot{\theta}_1$, $\dot{\theta}_2$: Rotational speed of the two driving wheels;

α: Angle between Cx' and CG;

γ: Angle between CG and the Cy';

$2b$: Distance between the two driving wheels;

$2a$: Length of the wheeled mobile robot;

d: Distance between the COG and the geometrical center.

Using the coordinate system shown in Figure 2, a kinematic analysis was carried out for the two-input, three-output nonlinear system. The kinematic equations are given as follows:

$$\begin{cases} \dot{x}_c = v_c \cos\phi \\ \dot{y}_c = v_c \sin\phi \end{cases} \tag{1}$$

$$\begin{bmatrix} v_c \\ \dot{\phi} \end{bmatrix} = \begin{bmatrix} \frac{r}{2} & \frac{r}{2} \\ \frac{r}{2b} & -\frac{r}{2b} \end{bmatrix} \begin{bmatrix} \dot{\theta}_1 \\ \dot{\theta}_2 \end{bmatrix} \tag{2}$$

where r is the radius of the two driving wheels.

The Lagrange formulation is used to derive the dynamic equations for the mobile robot. Because the robot is constrained to the horizontal plane, its potential energy is 0. Considering COG shifts and load changes caused by the large loads, the kinematic energy of the robot is given as follows:

$$E = \frac{(M+m)}{2}(\dot{x}_g^2 + \dot{y}_g^2) + \frac{I + d^2(M+m)}{2}\dot{\phi}^2 + \frac{J_\omega + k^2 J_0}{2}(\dot{\theta}_1^2 + \dot{\theta}_2^2) \tag{3}$$

where M is the mass of the mobile robot; m is the equivalent mass that the load imposes on the mobile robot; d is the distance between the COG and the geometrical center; I is the moment of inertia of the wheeled mobile robot; J_ω is the moment of inertia of the driving wheels, J_0 is the moment of inertia of the driving motors, and k is the gear ratio. m and d vary with the weight and position of the loads.

According to the Lagrange formulation, the driving torques τ_1 and τ_2 acting upon the two wheels are given as follows:

$$\tau_i = \frac{d}{dt}\left[\frac{\partial E}{\partial \dot{\theta}_i}\right] - \frac{\partial E}{\partial \theta_i}, \quad (i = 1, 2) \tag{4}$$

Then, we can obtain the dynamic equations considering the nonlinear friction as follows:

$$\begin{cases} \tau_1 = m_{11}\ddot{\theta}_1 + m_{12}\ddot{\theta}_2 + T_1(\dot{\theta}_1) \\ \tau_2 = m_{21}\ddot{\theta}_1 + m_{22}\ddot{\theta}_2 + T_2(\dot{\theta}_2) \end{cases} \tag{5}$$

where $\ddot{\theta}_1$ and $\ddot{\theta}_2$ denote the acceleration of the two wheels, and

$$m_{11} = \frac{r^2(M+m)}{4b^2}(b + d\cos\alpha)^2 + \frac{r^2[I + d^2(M+m)]}{4b^2} + (J_\omega + k^2 J_0)$$

$$m_{12} = \frac{r^2(M+m)}{4b^2}(b + d\cos\alpha)(b - d\cos\alpha) - \frac{r^2[I + d^2(M+m)]}{4b^2}$$
$$m_{21} = m_{12}$$
$$m_{22} = \frac{r^2(M+m)}{4b^2}(b - d\cos\alpha)^2 + \frac{r^2[I + d^2(M+m)]}{4b^2} + (J_\omega + k^2 J_0)$$

$T_1(\dot{\theta}_1)$ and $T_2(\dot{\theta}_2)$ denote the nonlinear friction torques of the two wheels, which are given as follows:

$$T_i(\dot{\theta}_i) = T_{vi}(\dot{\theta}_i) + T_{ci}(\dot{\theta}_i), \quad (i = 1, 2) \tag{6}$$

where $T_{vi}(\dot{\theta}_i)$ is the viscous friction, which is given as

$$T_{vi}(\dot{\theta}_i) = c_i\dot{\theta}_i \tag{7}$$

where c_i is the viscous friction coefficient, and $T_{ci}(\dot{\theta}_i)$ is the sum of coulomb friction and stribeck friction. $T_{ci}(\dot{\theta}_i)$ is given as

$$T_{ci}(\dot{\theta}_i) = \begin{cases} \tau_i & \dot{\theta}_i = 0 \text{ and } \tau_i < T_{\max i} \\ T_{\max i} & \dot{\theta}_i = 0 \text{ and } \tau_i \geq T_{\max i} \\ T_{\min i} + (T_{\max i} - T_{\min i})e^{-a_i\dot{\theta}_i} & \dot{\theta}_i > 0 \\ -T_{\min i} + (T_{\min i} - T_{\max i})e^{a_i\dot{\theta}_i} & \dot{\theta}_i < 0 \end{cases} \tag{8}$$

where $T_{\max i}$ is the maximum static friction, and $T_{\min i}$ is the coulomb friction, a_i is the stribeck friction coefficient. In simulation, the friction coefficients in (6) are assigned to different values to imitate the different ground conditions in order to verify the effectiveness of the proposed control method. It can be seen from the kinematic Equations (1), (2) and the dynamic Equations (5) that the mobile robot has three output variables x_c, y_c and ϕ controlled by two independent inputs τ_1 and τ_2. The system is a nonlinear system with nonlinear friction.

3. **Control Design.** In this section, an digital acceleration control method is developed for the wheeled mobile robot [9]. To derive control law for the system, the dynamic Equations (5) are rewritten in matrix form as

$$\boldsymbol{\tau} = \boldsymbol{M}\ddot{\boldsymbol{\theta}} + \boldsymbol{T}(\dot{\boldsymbol{\theta}}) \tag{9}$$

where

$$\boldsymbol{\tau} = [\ \tau_1 \quad \tau_2\ ]^T, \quad \ddot{\boldsymbol{\theta}} = [\ \ddot{\theta}_1 \quad \ddot{\theta}_2\ ]^T$$
$$\boldsymbol{M} = \begin{bmatrix} m_{11} & m_{12} \\ m_{21} & m_{22} \end{bmatrix}$$
$$\boldsymbol{T}(\boldsymbol{\theta}) = [\ T_1(\dot{\theta}_1) \quad T_2(\dot{\theta}_2)\ ]^T$$

Firstly, the value of the control torque is kept constant between every time period of length T by a zero-order holder device, as shown in Figure 3. Here, T is the sampling interval of the digital control torque and kT^+ is the instant after the change of the control torque at time kT.

For a constant sampling period T, for times kT^+ and kT, we can obtain (10) from (9) as

$$\begin{aligned} \boldsymbol{\tau}[kT] &= \boldsymbol{M}\ddot{\boldsymbol{\theta}}(kT) + \boldsymbol{T}[\dot{\boldsymbol{\theta}}(kT)] \\ \boldsymbol{\tau}[kT^+] &= \boldsymbol{M}\ddot{\boldsymbol{\theta}}(kT^+) + \boldsymbol{T}[\dot{\boldsymbol{\theta}}(kT^+)] \end{aligned} \tag{10}$$

where $\boldsymbol{\tau}[kT] = \boldsymbol{\tau}[(k-1)T^+]$ is the control torque during $[(k-1)T^+, kT]$, and $\boldsymbol{\tau}[kT^+]$ is the control torque to be designed during $[kT^+, (k+1)T]$. As shown in Figure 3, when the control torque is changed at time kT^+, the acceleration is changed; however, the

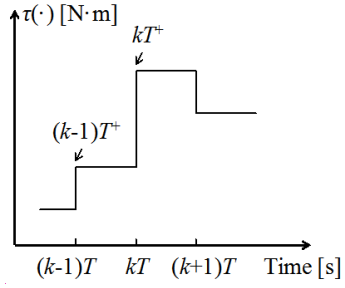

FIGURE 3. Stepwise change of control force

velocity, position and nonlinear friction are still the same by integral characteristic, which are shown in (11).

$$\begin{aligned} \ddot{\boldsymbol{\theta}}(kT^+) &\neq \ddot{\boldsymbol{\theta}}(kT) \\ \dot{\boldsymbol{\theta}}(kT^+) &= \dot{\boldsymbol{\theta}}(kT) \\ \boldsymbol{\theta}(kT^+) &= \boldsymbol{\theta}(kT) \\ \boldsymbol{T}(kT^+) &= \boldsymbol{T}(kT) \end{aligned} \tag{11}$$

At time kT^+, the mobile robot tracks the designed path $\boldsymbol{\theta}^*(kT^+)$; therefore, in Equation (10), the $\ddot{\boldsymbol{\theta}}(kT^+)$ in control torque $\boldsymbol{\tau}(kT^+)$ is set to be $\ddot{\boldsymbol{\theta}}^*(kT)$. Considering the compensation of original error and based on Equation (10), the control input at time kT^+ is designed as follows:

$$\begin{aligned} \boldsymbol{\tau}(kT^+) = \boldsymbol{\tau}[(k-1)T^+] + \boldsymbol{M}\{&[\ddot{\boldsymbol{\theta}}^*(kT^+) - \ddot{\boldsymbol{\theta}}(kT)] \\ &+ \boldsymbol{K}_D[\dot{\boldsymbol{\theta}}^*(kT) - \dot{\boldsymbol{\theta}}(kT)] + \boldsymbol{K}_P[\boldsymbol{\theta}^*(kT) - \boldsymbol{\theta}(kT)]\} \end{aligned} \tag{12}$$

where $\boldsymbol{K}_D$, $\boldsymbol{K}_P$ are the parameters of the acceleration controller. $\boldsymbol{K}_D$ is the speed deviation coefficient and $\boldsymbol{K}_P$ is position deviation coefficient, respectively. Here, $\boldsymbol{K}_D$, $\boldsymbol{K}_P$ are diagonal positive-definite matrices shown as follows:

$$\boldsymbol{K}_D = \begin{bmatrix} k_{d1} & 0 \\ 0 & k_{d2} \end{bmatrix}, \quad \boldsymbol{K}_P = \begin{bmatrix} k_{p1} & 0 \\ 0 & k_{p2} \end{bmatrix}$$

Let the tracking error be

$$\boldsymbol{e}(kT^+) = \boldsymbol{\theta}^*(kT^+) - \boldsymbol{\theta}(kT^+) \tag{13}$$

Substituting into (12) using (10), (11) and (13) yields

$$\ddot{\boldsymbol{e}}(kT^+) + \boldsymbol{K}_D\dot{\boldsymbol{e}}(kT^+) + \boldsymbol{K}_P\boldsymbol{e}(kT^+) = 0 \tag{14}$$

In the short time interval of $[kT^+, (k+1)T]$, Equation (15) holds.

$$\begin{aligned} \dot{\boldsymbol{e}}[(k+1)T^+] &= \dot{\boldsymbol{e}}(kT^+) + \ddot{\boldsymbol{e}}(kT^+)T \\ \boldsymbol{e}[(k+1)T^+] &= \boldsymbol{e}(kT^+) + \dot{\boldsymbol{e}}(kT^+)T + \ddot{\boldsymbol{e}}(kT^+)T^2/2 \end{aligned} \tag{15}$$

Using (14) and (15) we can obtain

$$\begin{bmatrix} \boldsymbol{e}[(k+1)T^+] \\ \dot{\boldsymbol{e}}[(k+1)T^+] \end{bmatrix} = \boldsymbol{A} \begin{bmatrix} \boldsymbol{e}[kT^+] \\ \dot{\boldsymbol{e}}[kT^+] \end{bmatrix} \tag{16}$$

where

$$\boldsymbol{A} = \begin{bmatrix} \boldsymbol{I} - \boldsymbol{K}_P T^2/2 & (\boldsymbol{I} - \boldsymbol{K}_D T/2)T \\ -\boldsymbol{K}_P T & \boldsymbol{I} - \boldsymbol{K}_D T \end{bmatrix}$$

Here, $\boldsymbol{K}_D$, $\boldsymbol{K}_P$ are designed to ensure that all eigenvalues of $\boldsymbol{A}$ are within the unit circle. Then, we can obtain

$$\lim_{k\to\infty} \boldsymbol{e}(kT) = \lim_{k\to\infty} [\boldsymbol{\theta}^*(kT) - \boldsymbol{\theta}(kT)] = 0 \tag{17}$$

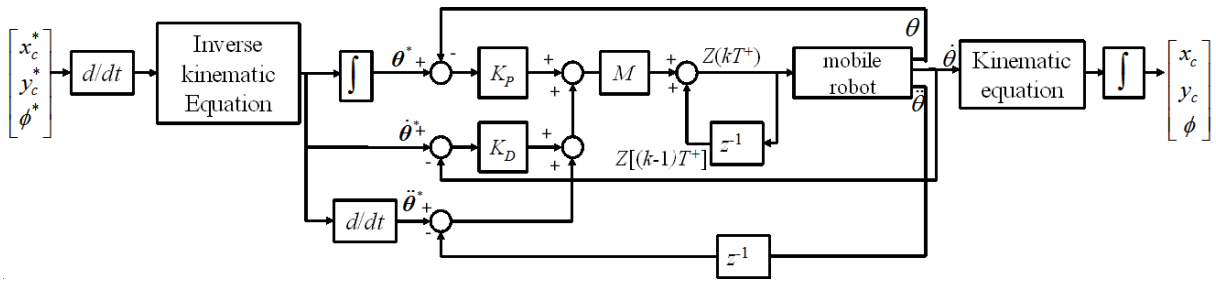

FIGURE 4. Block diagram of the digital acceleration control system

Therefore, the system is stable, that is, $\lim_{k\to\infty} \boldsymbol{\theta}(kT) = \boldsymbol{\theta}^*(kT)$. Furthermore, the following equation is obtained:

$$\begin{aligned} \lim_{k\to\infty} x_c &= x_c^* \\ \lim_{k\to\infty} y_c &= y_c^* \\ \lim_{k\to\infty} \phi &= \phi^* \end{aligned} \tag{18}$$

Therefore, the path-tracking is accomplished. Figure 4 shows the block diagram of the control system.

4. **Simulation.** In this section, to verify the effectiveness of digital acceleration control to deal with the COG shifts, load changes, and nonlinear friction, simulations are conducted comparing with a PI controller. The dynamic model shown in (5) is used in the simulation. The physical parameters of the mobile robot in the simulation are given below.
$M = 46.5$ kg, $m = 60$ kg, $b = 0.27$ m, $d = 0.2$ m, $r = 0.122$ m, $I = 1.3133$ kg·m^2, $\gamma = \pi/6$ rad, $\alpha = 2\pi/3$ rad, $c_1 = c_2 = 0.2$ kg·m^2/s, $a_1 = a_2 = 500$ m^2/s, $T_{\max 1,2} = 60$ N·m, $T_{\min 1,2} = 6$ N·m, $J_0 = 0.0125$ kg·m^2, $J_\omega = 0.0144$ kg·m^2 and $k = 3$.

As usual, the cargo-transport task requires the mobile robot to automatically move from a start position to a target position following a predefined path. The predefined path consists of a series of circular and linear path. Here, to thoroughly verify the tracking performance of the proposed control method, we assume that the mobile robot follows a circular path. To ensure the reliability and safety of the robot and cargo, we design a smooth path with soft acceleration and deceleration, the start and stop speed is set to 0. The circular trajectory to follow is described by

$$\begin{aligned} x_c^*(t) &= x_0 + r\cos\sigma(t) \\ y_c^*(t) &= y_0 + r\sin\sigma(t) \\ \phi^*(t) &= \tfrac{\pi}{2} + \sigma(t) \end{aligned} \tag{19}$$

where

$$\sigma(t) = \begin{cases} \frac{4\pi}{t_0^2}t^2 & 0 \le t \le \frac{t_0}{2} \\ 2\pi - \frac{4\pi}{t_0^2}(t-t_0)^2 & \frac{t_0}{2} \le t \le t_0 \end{cases}$$

$(x_0, y_0) = (5\text{ m}, 5\text{ m})$ specifies the center of the circle, $r = 4$ m is the radius, the parameter t_0 can be changed to modify the moving speed of the mobile robot, here t_0 is set to be 150 s. The simulation time is 150 s. The initial position $x_c(0) = 8$ m, $y_c(0) = 4$ m and the initial angle $\phi(0) = 0$ rad.

4.1. **Simulation of PI controller.** The PI control input is described as follows:

$$\begin{aligned} \tau_1 &= k_{p1}(\theta_1^* - \theta_1) + k_{i1}\int(\theta_1^* - \theta_1)dt \\ \tau_2 &= k_{p2}(\theta_2^* - \theta_2) + k_{i2}\int(\theta_2^* - \theta_2)dt \end{aligned} \tag{20}$$

where, k_{p1} and k_{p2} are the proportional gain parameters; k_{i1} and k_{i2} are the integral gain parameters of the two control inputs respectively. The parameters of the PI controller are adjusted in the simulation assuming no nonlinear friction ($\boldsymbol{T}(\dot{\boldsymbol{\theta}}) = 0$), the COG shifts and load changes are considered that is $\alpha = 2\pi/3$ rad, $d = 0.2$, $m = 80$ kg. The parameters of the PI controller are given as $k_{p1} = k_{p2} = 1$; $k_{i1} = k_{i2} = 3$.

Figures 5(a1) – 5(d1) show the tracking performance of the mobile robot for the x position, y position, time-variant orientation angle ϕ, and the tracking and gradient when assuming no nonlinear friction ($\boldsymbol{T}(\dot{\boldsymbol{\theta}}) = 0$), using the PI controller. This is compared with Figures 5(a2) – 5(d2), which show the tracking performance of the mobile robot when nonlinear friction exists ($\boldsymbol{T}(\dot{\boldsymbol{\theta}}) \neq 0$), with no changes to the other parameters. In Figure

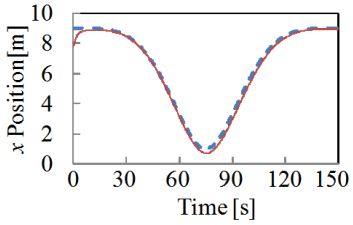

(a1) x position $\boldsymbol{T}(\dot{\boldsymbol{\theta}}) = 0$ N·m

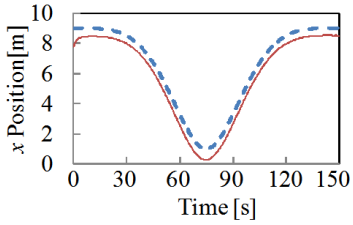

(a2) x position $\boldsymbol{T}(\dot{\boldsymbol{\theta}}) \neq 0$ N·m

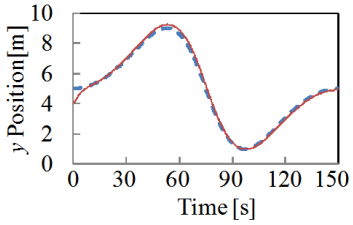

(b1) y position $\boldsymbol{T}(\dot{\boldsymbol{\theta}}) = 0$ N·m

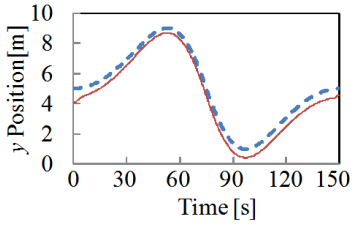

(b2) y position $\boldsymbol{T}(\dot{\boldsymbol{\theta}}) \neq 0$ N·m

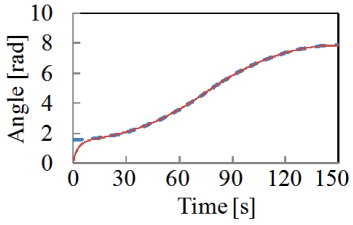

(c1) Orientation angle $\boldsymbol{T}(\dot{\boldsymbol{\theta}}) = 0$ N·m

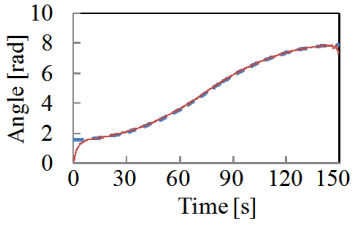

(c2) Orientation angle $\boldsymbol{T}(\dot{\boldsymbol{\theta}}) \neq 0$ N·m

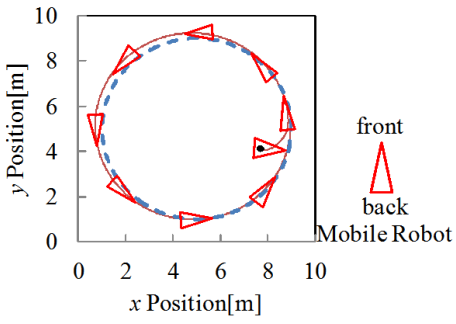

(d1) Tracking and gradient results $\boldsymbol{T}(\dot{\boldsymbol{\theta}}) = 0$ N·m

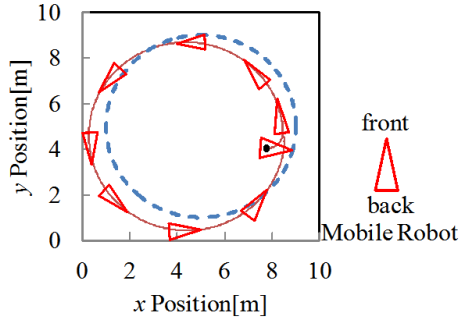

(d2) Tracking and gradient results $\boldsymbol{T}(\dot{\boldsymbol{\theta}}) \neq 0$ N·m

FIGURE 5. Simulation results of the PI controller

5, the dotted line represents the reference, and the solid line represents the PI control response, the COG shifts and load changes are considered.

When assuming no nonlinear friction, as shown in Figures 5(a1) – 5(c1), the PI control method has good performance tracking for the x position, y position, and time-variant orientation angle ϕ when $\boldsymbol{T}(\dot{\boldsymbol{\theta}}) = 0$. Figure 5(d1) shows, for this case, the mobile robot could almost track the target trajectory, which have a small tracking error.

On the contrast, when nonlinear friction is added, in Figures 5(a2) – 5(b2), the system has x position and y position errors. In Figure 5(c2), an orientation angle error occurs after 140 s. Figure 5(d2) shows that the mobile robot system cannot track the target trajectory. Figures 5(a2) – 5(d2) indicate that the mobile robot system cannot track the target trajectory using the PI controller when nonlinear friction is added. These simulation results demonstrate that the PI control method is only effective when friction is assumed to 0 by properly tuning the parameters. However, when the nonlinear friction is added, the PI control method is not effective anymore.

4.2. **Simulation result of digital acceleration controller.** The parameters of the digital acceleration controller are adjusted in the simulation, assuming no nonlinear friction ($\boldsymbol{T}(\dot{\boldsymbol{\theta}}) = 0$), considering COG shifts and load changes. The parameters of digital acceleration controller are given as follows:

$$\boldsymbol{K}_D = \begin{bmatrix} k_{d1} & 0 \\ 0 & k_{d2} \end{bmatrix} = \begin{bmatrix} 3 & 0 \\ 0 & 3 \end{bmatrix} s^{-1}$$

$$\boldsymbol{K}_P = \begin{bmatrix} k_{p1} & 0 \\ 0 & k_{p2} \end{bmatrix} = \begin{bmatrix} 0.6 & 0 \\ 0 & 0.6 \end{bmatrix} s^{-2}$$

Figures 6 (a1) – 6(d1) show the tracking performance of the mobile robot for the x position, y position, time-variant orientation angle ϕ, and the tracking and gradient when assuming no nonlinear friction ($\boldsymbol{T}(\dot{\boldsymbol{\theta}}) = 0$), using the proposed digital acceleration algorithm. This is compared with Figures 6(a2) – 6(d2), which show the tracking performance of the mobile robot when nonlinear friction exists ($\boldsymbol{T}(\dot{\boldsymbol{\theta}}) \neq 0$), with no changes to the other parameters. In Figures 6, the dotted line represents the reference, and the solid line represents the digital acceleration control response, the COG shifts and load changes are considered that is $\alpha = 2\pi/3$ rad, $d = 0.2$, $m = 80$ kg. In Figures 6(a1) – 6(c1) and Figures 6(a2) – 6(c2), the horizontal axes is simulation time, for a simulation time of 150 s, and the vertical axes are x position, y position, and orientation angle, respectively. Figure 6(d1) and Figure 6(d2) show the tracking and gradient of the mobile robot.

As shown in Figures 6(a1) – 6(d1), the digital acceleration control method has good tracking performance for the x position, y position, and time-variant orientation angle ϕ for $\boldsymbol{T}(\dot{\boldsymbol{\theta}}) = 0$, for this case, the mobile robot can have a good trajectory tracking performance. In Figures 6(a2) – 6(d2), the response curves are similar to those in Figures 6(a1) – 6(d1), which indicates that the proposed digital acceleration algorithm allows good tracking performance for the x position, y position, and time-variant orientation ϕ even if nonlinear friction exists in the system with no change to the control parameters. In theory, the digital acceleration controller is effective to deal with a wide range of uncertain or unbounded nonlinear friction when the input torque is limitless. In the simulations, the parameters of the nonlinear friction in (8) are assigned to different values to represent the different type and scope of nonlinear friction. The simulation results are almost the same as the results in Figure 6, which are in good agreement to theoretical analysis.

The above simulation results show that the proposed digital acceleration control method is more feasible and effective to deal with the uncertain and unbounded nonlinear friction than the PI control when COG shifts and load changes are considered. The current control

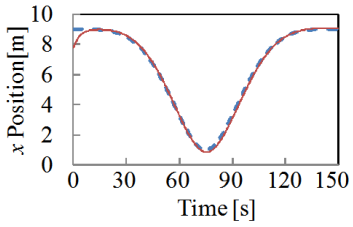

(a1) x position $\boldsymbol{T}(\dot{\boldsymbol{\theta}}) = 0$ N·m

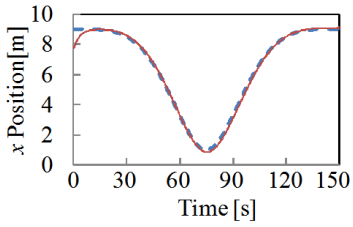

(a2) x position $\boldsymbol{T}(\dot{\boldsymbol{\theta}}) \neq 0$ N·m

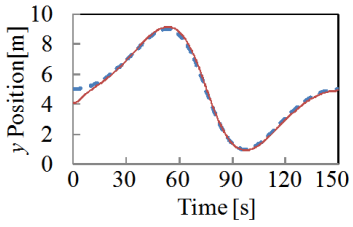

(b1) y position $\boldsymbol{T}(\dot{\boldsymbol{\theta}}) = 0$ N·m

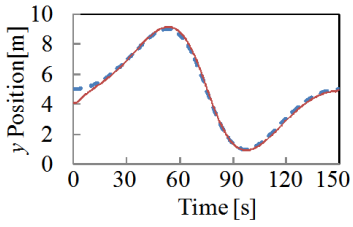

(b2) y position $\boldsymbol{T}(\dot{\boldsymbol{\theta}}) \neq 0$ N·m

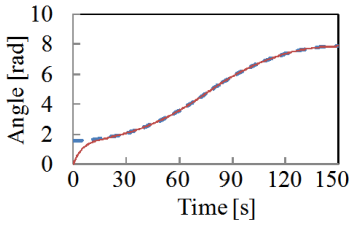

(c1) Orientation angle $\boldsymbol{T}(\dot{\boldsymbol{\theta}}) = 0$ N·m

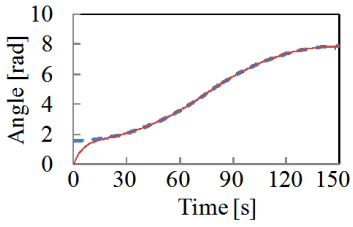

(c2) Orientation angle $\boldsymbol{T}(\dot{\boldsymbol{\theta}}) \neq 0$ N·m

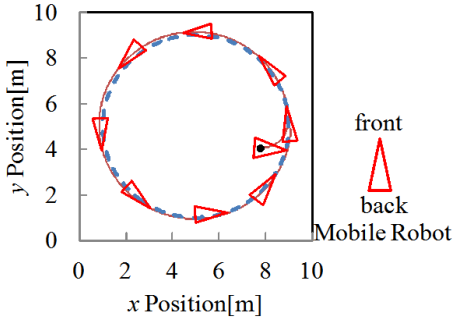

(d1) Tracking and gradient results $\boldsymbol{T}(\dot{\boldsymbol{\theta}}) = 0$ N·m

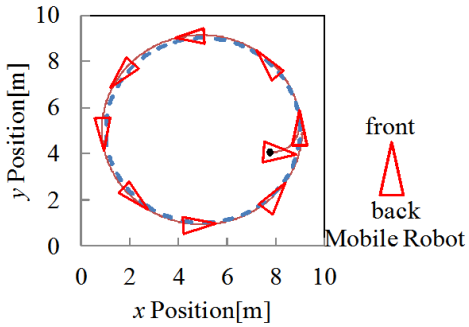

(d2) Tracking and gradient results $\boldsymbol{T}(\dot{\boldsymbol{\theta}}) \neq 0$ N·m

FIGURE 6. Simulation results of the proposed digital acceleration controller

torque can compensate for nonlinear friction by using the previous sampling period's acceleration signal, because the previous sampling period's acceleration signal includes the effect of previous sampling period's nonlinear friction, and the current friction is almost the same as the previous sampling period's friction. Therefore, the proposed digital acceleration controller can allow the controlled system to compensate for a greater scope of nonlinear friction, which was verified by the simulations.

5. **Conclusions.** In this paper, a digital acceleration control method is proposed for the path-tracking of a wheeled mobile robot to deal with COG shifts, load changes, and the uncertain and unbounded nonlinear friction. Compared with a PI controller, the feasibility and effectiveness of the proposed control method is demonstrated by circular path-tracking simulations.

Future work will focus on applying the proposed digital acceleration control algorithm in the path tracking experiment of the mobile robot.

REFERENCES

[1] S. Hoshino, H. Seki, Y. Naka and J. Ota, Fault-tolerant multi-robot operational strategy for material transport systems considering maintenance activity, *Journal of Robotics and Mechatronics*, vol.22, no.4, pp.485-495, 2010.

[2] M. Minami, T. Ikeda and M. Takeuchi, Dynamic model of mobile robot including slipping of carrying objects, *International Journal of Innovative Computing, Information and Control*, vol.3, no.2, pp.353-369, 2007.

[3] C. C. de Wit, Trends in mobile robot and vehicle control, in *Control Problems in Robotics*, B. Siciliano and K. P. Valavanis (eds.), London, U.K., Springer-Verlag, 1998.

[4] M. Egerstedt, X. Hu and A. Stotsky, Control of a car-like robot using a dynamic model, *Proc. of the 1998 IEEE International Conference on Robotics and Automation*, Leuven, Belgium, vol.4, pp.3273-3278, 1998.

[5] Z. P. Jiang and J. B. Pomet, Combining backstepping and time-varying techniques for a new set of adaptive controllers, *Proc. of the 33rd IEEE Conf. on Decision and Control*, Lake Buena Vista, FL, USA, pp.2207-2212, 1994.

[6] R. T. M'Closkey and R. M. Murray, Exponential stabilization of driftless nonlinear control systems via time-varying, homogeneous feedback, *Proc. of the 33rd IEEE Conf. on Decision and Control*, vol.2, pp.1317-1322, 1994.

[7] S. Y. Wang, T. Tsuchiya and Y. Hashimoto, The digital acceleration control method of robot manipulator, *Proc. of the 1st Symposium on Robot Robotics Society of Japan*, vol.1, pp.7-12, 1991 (in Japanese).

[8] S. Y. Wang, T. Tsuchiya and Y. Hashimoto, Path tracking control of robot manipulators utilizing future information of desired trajectory, *Transactions of the Japan Society of Mechanical Engineers*, vol.59, no.564C, pp.2512-2518, 1993 (in Japanese).

[9] T. Tsuchiya and K. Fukaya, *Introduction of Mechatronics*, Morikita Publishing Co, Tokyo, 2004.

[10] Y. N. Wang, S. Y. Wang, R. P. Tan and Y. L. Jiang, Digital acceleration control method for path tracking control of an autonomous mobile robot, *ICIC Express Letters, Part B: Applications*, vol.2, no.6, pp.1267-1272, 2011.